

Descriptors for thermal expansion in solids

Joseph T. Schick,^{1,*} Abhijith M. Gopakumar,² and Andrew M. Rappe²

¹*Department of Physics, Villanova University, Villanova, PA 19085, USA*

²*Department of Chemistry, University of Pennsylvania, Philadelphia, PA 19104, USA*

(Dated: January 17, 2017)

Abstract

Thermal expansion in materials can be accurately modeled with careful phonon calculations within density functional theory. However, because of interest in controlling thermal expansion and the time consumed evaluating thermal expansion properties of candidate materials, either theoretically or experimentally, an approach to rapidly identifying materials with desirable thermal expansion properties would be of great utility. We show that the fraction of crystal volume occupied by ions, based upon ionic radii, the deviation of bond coordination divided by mean bond coordination, and the ratio of least to greatest atomic mass are descriptors that correlate with the coefficient of thermal expansion for a variety of materials found in widely accessible databases. Correlation is greatly improved by combining these descriptors in a multi-dimensional quadratic fit. Open space combined with a range of atomic masses and a variety of local bond coordinations indicates materials with lower coefficients of thermal expansion. Materials with single-valued local coordination and less open space have the highest coefficients of thermal expansion.

I. INTRODUCTION

Because of the potential for temperature gradients or other thermal stresses to cause electronic devices to fail, knowledge of the coefficients of thermal expansion (CTE) of materials is important. Either active materials with desired thermal properties or composites of active and compensating materials can mitigate the ill effects of thermal expansion in real devices.^{1,2} A compensating material must be chemically and electrically compatible with the functional material and will typically contract with increasing temperature; i.e. it will exhibit negative thermal expansion (NTE). While the CTE for many materials have been cataloged, the set of known NTE materials is small, and materials appropriate for specific applications may not yet be available. A means of rapidly predicting the thermal expansion properties of yet-to-be investigated materials will be extremely useful.

The displacement of the equilibrium positions of atoms in a material with temperature is the source of thermal expansion. While anharmonicity in the vibrations of bonded pairs of atoms will drive the atoms farther apart with increasing temperature, crystal structure also plays an essential role in the specific thermal expansion characteristics of a material, providing behaviors over the range from positive thermal expansion (PTE) to NTE. Accurate theoretical modeling of thermal expansion in materials necessitates quantum mechanical calculations and dynamical calculations or, minimally, quasi-harmonic modeling. As a result, typical calculations of thermal expansion address the microscopic causes of experimentally-observed CTE on a case-by-case basis. Especially prevalent recently are experimental and theoretical investigations of materials that exhibit NTE, such as ZrW_2O_8 ,³⁻¹⁵ $M_2\text{O}$ (with $M = \text{Cu, Ag, Au}$),¹⁶ ReO_3 ,^{17,18} and ScF_3 .^{19,20} Except for materials with very similar electronic and structural properties, a global picture capable of guiding searches for new materials with desired thermal expansion characteristics is slow to emerge. Comprehensive reviews of thermal expansion in materials, emphasizing NTE in both theory and experiment, can be found in Refs. 21 and 22.

For microscopic atomic displacements to create NTE, the motions of the atoms must carry them into spaces already existing within the lattice, while simultaneously drawing neighboring ions closer together. It is well-known^{21,22} that the definition of CTE,

$$\text{CTE} = \frac{1}{V} \left(\frac{\partial V}{\partial T} \right)_P, \quad (1)$$

can, with the help of a Maxwell relation, be rewritten as

$$\text{CTE} = -\frac{1}{V} \left(\frac{\partial S}{\partial P} \right)_T, \quad (2)$$

which shows that for a material to exhibit NTE, entropy must increase with pressure, contrary to typical expectations. Decreasing the volume available to a particle, e.g. by increasing pressure, is associated with decreasing entropy. The definition in Eq. 2 is isothermal which effectively means that the momentum space contribution to entropy changes negligibly relative to the real space contribution. From this we deduce that applying pressure in an NTE material increases the volume available to its constituent atoms. On the other hand, applying pressure to PTE materials (at constant temperature) results in decreasing entropy, implying a corresponding decrease in the volume available to the atoms follows from the same line of argument used above. In order for there to be more volume available to the atoms within a crystalline material under increasing pressure, atomic motions must be directed more significantly into the open spaces within the lattice. In other words, the atomic motions possess significant components in directions perpendicular to the bonds with nearest neighbor atoms. The difference between NTE and PTE is therefore quantifiable by the degree to which ionic thermal displacements are longitudinal or transverse with respect to the bonds. Experimental evidence supporting this view is found, for example, in a study of NTE in ScF_3 , in which inelastic neutron scattering shows that the Sc-F bonds lengthen with increasing temperature and that the material contracts over a wide temperature range as a result of large transverse motions of the F ions.¹⁹ In our recent molecular dynamics investigation we demonstrated that thermal expansion in a single structure, with expanding bonds modeled with first- and second-neighbor interactions via Morse potentials, can be varied from NTE to PTE by increasing the second-neighbor interaction strength relative to the first-neighbor interactions.²³ By adjusting second-neighbor interactions, we reduced the transverse motions of the light ions, resulting in the emergence of PTE in the model.

We propose that an approach to predicting thermal expansion can be found by scanning the literature for the structures of crystals, focusing on quantities that may have a relationship to the entropy of the material and its potential to increase or decrease with respect to pressure, such as the space occupied by ions, their coordinations, and the distribution of atomic masses. We employ the wealth of structural information in databases such as the Inorganic Crystal Structure Database (ICSD)^{24,25} and the Crystallographic Open Database

(COD)^{26–30} in this work. By correlating materials with known CTE to their structures, we can begin to determine useful descriptors for thermal expansion. In Section II, we discuss the physical underpinnings for the quantities that we propose for descriptors of CTE. In Section III, we present the choice of descriptors from the original list of quantities of interest along with the result of performing a fit using the descriptors developed. We conclude with a discussion of the implications this correlation will have in the search for materials with desired thermal expansion properties.

II. PROPOSED DESCRIPTORS

For each atom in a unit cell of each material, the number of nearest neighbors and formal oxidation state are determined. From this information we obtain ionic radii³¹ r_i for each ion and an estimate of the volume each ion occupies (assuming it occupies a sphere of volume $V_i = \frac{4}{3}\pi r_i^3$). The fractional volume occupied is the total volume estimated for all the atoms in the unit cell divided by the volume of the unit cell $V_{\text{u.c.}}$:

$$v = \frac{1}{V_{\text{u.c.}}} \sum_i V_i. \quad (3)$$

A complete list of the data used for this investigation is provided in the Appendix. As seen in Fig. 1, thermal expansion data for the materials we sampled shows there is a relationship between thermal expansion and the volume occupied by atoms in the lattice; more open space corresponds to a greater likelihood for NTE.

The cluster of points with CTE $\gtrsim 30 \times 10^{-6}/\text{K}$ in Fig. 1 consists of binary materials that have the rock salt structure, with the corresponding high coordination providing an explanation for the large positive thermal expansion in these materials. We note that Coulomb interactions between second neighbors will be repulsive and strong. The data point with the highest volume occupied and very low PTE belongs to BN. Because of its zincblende structure, the B and N atoms in BN have tetrahedral coordination. We also note that BN has a high bulk modulus, which implies that the tetrahedral bonds are strong. However, the low CTE of BN suggests that ionic thermal motions are mostly directed into open spaces which are available because of low coordination. We deduce from this that bond coordination in a material is a possible descriptor to predict thermal expansion coefficients. Finally, for some materials that exhibit negative thermal expansion, it has been noted that motion of

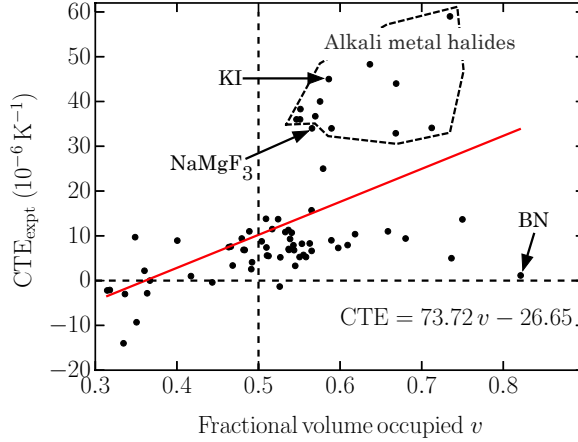


FIG. 1. (Color online) The experimental coefficient of thermal expansion (CTE) is plotted as a function of fractional volume occupied as defined in Eq. 3 for the materials gleaned from the literature. Apparently, NTE is possible only when v is less than ≈ 0.5 . The trend in the data is highlighted with a linear fit. The data with expansion coefficients greater than $30 \times 10^{-6} \text{ K}^{-1}$ are ionic solids in the rock salt structure. The RMS deviation between the data and the fit is $\approx 12.5 \times 10^{-6} \text{ K}^{-1}$ and the correlation coefficient is 0.53.

light ions in the directions transverse to their bonds is at the root of their atypical thermal expansion. One underlying reason for this is that lighter ions undergo greater amplitude of motion than their heavier counterparts, which will assist the emergence of NTE provided there exist open spaces and low coordinations around the light ions. Therefore, we include atomic mass in the list of potential descriptors.

III. RESULTS AND DISCUSSION

Quantities extracted in the search for descriptors, in addition to v , are the mean bond coordination $\langle c \rangle$, its standard deviation σ_c , the mean atomic mass $\langle m \rangle$, the minimum mass m , the maximum mass M , and the standard deviation of mass σ_m . In Fig. 2, we display the linear correlations between descriptor candidates and the experimental CTE. In addition, we include unitless ratios $\sigma_c/\langle c \rangle$, $\sigma_m/\langle m \rangle$, and the ratio of minimum to maximum mass m/M . The quantities that have the strongest correlations with the CTE are v and $\langle c \rangle$, with correlations 0.53 and 0.57, respectively. These two candidates correlate strongly with

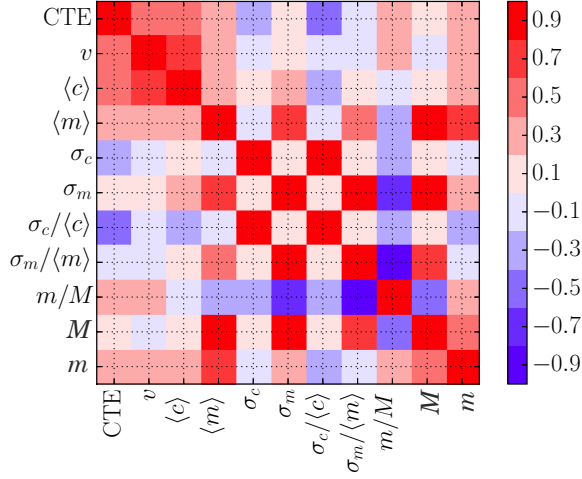


FIG. 2. (Color online) The correlations (Pearson- r) between candidate descriptors and the coefficient of thermal expansion CTE for 69 materials taken from the literature. Moderate linear correlation with CTE is found for both the mean coordination and occupied volume. Weak-to-moderate correlation is exhibited by both the mean mass and the ratio of minimum to maximum atomic mass. Cross correlations between descriptors permit identification of more nearly independent descriptors: the occupied volume, the ratio of the standard deviation to the mean coordination, and the ratio of minimum to maximum mass.

each other; little is to be gained from using them together. The next-most-highly correlated quantity is $\sigma_c/\langle c \rangle$, with a (negative) correlation of -0.47 to the CTE. Furthermore, this quantity has a low degree of correlation with the volume ratio v , making it a better quantity for using jointly with v to predict CTE. The candidates for mass have lower correlations with the CTE. The ratio of minimum to maximum atomic mass correlation with CTE is 0.25 and cross-correlates only moderately with v and $\sigma_c/\langle c \rangle$. From our search for moderate-to-strong correlations with CTE and weak-to-moderate cross-correlations, we determine v , $\sigma_c/\langle c \rangle$, and m/M to be a good set of descriptors. These quantities have the additional advantages of being unitless and possessing values between zero and one for all materials in our list, simplifying analysis of their fitting strengths.

We performed a second-order polynomial fit using these three descriptors and the 69

TABLE I. The parameters used in Eq. 4 to evaluate $\text{CTE}_{\text{calc}}(v, \sigma_c/\langle c \rangle, m/M)$.

i	j	k	c_{ijk}
0	0	0	-99.90
1	0	0	366.27
0	1	0	29.98
0	0	1	-2.66
1	1	0	-157.51
1	0	1	-183.38
0	1	1	6.24
2	0	0	-199.45
0	2	0	49.30
0	0	2	114.83

materials in our data sample, using the relation

$$\text{CTE}_{\text{calc}}\left(v, \frac{\sigma_c}{\langle c \rangle}, \frac{m}{M}\right) = \sum_{i+j+k \leq 2} c_{ijk} v^i \left(\frac{\sigma_c}{\langle c \rangle}\right)^j \left(\frac{m}{M}\right)^k. \quad (4)$$

The correlation plot for this fit is displayed in Fig. 3 and the coefficients are listed in Table I. The correlation coefficient is 0.80 and the RMS-deviation between the fit and the data is $8.9 \times 10^{-6} \text{ K}^{-1}$, a noticeable improvement over the the fit displayed in Fig. 1, with outlying points more closely fit. Points to the right of the diagonal are ones for which the model predicts thermal expansion greater than the experimentally measured value. The previously noted deviation in BN has been reduced by a factor of ≈ 2 . The predicted values for the ionic solids have also been increased toward their experimental values. The material with largest positive deviation ($\text{CTE}_{\text{calc}} > \text{CTE}_{\text{expt}}$) is HfO_2 . The largest negative deviation arises for KI.

In order to visualize the model and to isolate ranges of the descriptors that characterize the CTE, we present contours of constant CTE_{calc} across the ranges of $\sigma_c/\langle c \rangle$ and m/M at fixed volume ratios $v = 0.3, 0.4, \dots, 0.8$ in Fig. 4. Superimposed on the contours are points indicating the descriptor values of data used in the fit, including volume ratios within ± 0.05 of the value of v displayed in the corresponding panel. As noted previously, materials with the lowest volume ratios are most-likely to have NTE. In panels (a) and (b) in Fig. 4 we see

that the NTE materials generally have mass ratios below 0.4 and coordination descriptors $\sigma_c/\langle c \rangle$ of between 0.2 and 0.5. In addition to open space, important contributors to NTE are atoms with a distribution of masses and a range of coordinations.

The majority of materials in this work have volume ratios around 0.5 – 0.6. These are displayed in panels (c) and (d) in Fig. 4. These materials also generally possess CTE that would be considered typical. As seen for the low-volume-ratio materials, the lower values of CTE_{calc} fall in the middle of the ranges of the coordination and mass descriptors, suggesting nonlinear dependence. Many of the materials here have zero coordination variance as a result of simple structures, such as rocksalt for which the atoms have identical coordination environments. A zero value in the coordination descriptor indicates the material has a high PTE value. Greater variance in the coordination indicates lower values of PTE.

The trend linking large PTE with low coordination descriptor values and lower CTE with larger values of the coordination descriptor continues into the most volume-crowded materials, which are seen in panels (e) and (f) of Fig. 4. Many of these materials have zero values of the coordination descriptor, indicating simple, high-coordination structures. The materials with lower CTE values either have mass ratios closer to 0.5 or have more complex bonding environments, as quantified by large coordination descriptor values.

The trends here indicate that materials that can be considered typical, with $\text{CTE} \approx 10 \times 10^{-6} \text{ K}^{-1}$, have volume ratios $0.45 \lesssim v \lesssim 0.6$, coordination descriptors $0.2 \lesssim \sigma_c/\langle c \rangle \lesssim 0.4$, and mass ratios $0.1 \lesssim m/M \lesssim 0.3$. A coordination descriptor ≈ 0 generally means large PTE. NTE requires low volume ratio and mid-range values for the other descriptors.

The CTE of BN and HfO_2 are both overestimated by the present description. In the case of BN, its zincblende structure means all atoms have tetrahedral coordination with zero variance, and its large ionic volume gives the material higher model CTE. We note that a number of materials with zincblende or diamond lattice structures, such as Si, show NTE for a range of low temperatures.³² A relatively low resistance for B-N-B (or Si-Si-Si) bond angles to change may account for the discrepancy between the model and experiment. The present model does not have a parameter that can access this particular characteristic. The reappearance of a zone of NTE in the middle-right in panels (e) and (f) of Fig. 4 is a result of including BN in the fit. Removing BN from the fit eliminates this NTE region and improves some values for the CTE at the high end of the volume ratio. HfO_2 is in the mid-range of volume and coordination descriptors but its mass ratio is very low, $m/M = 0.09$, which in

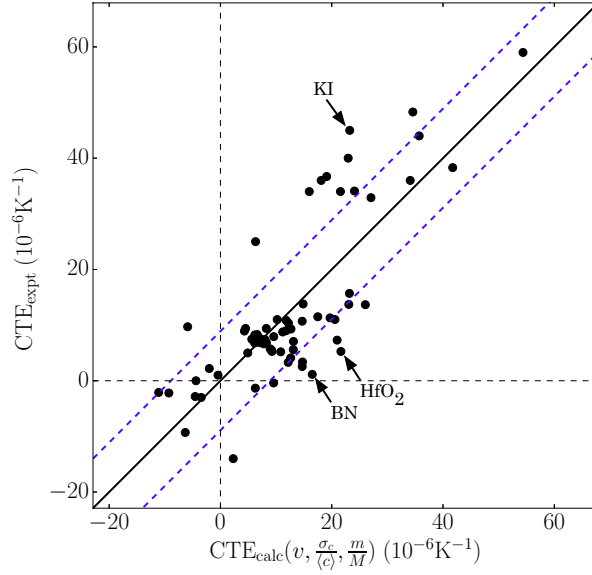


FIG. 3. (Color online) Correlation plot of experimental and calculated CTE generated by a two-parameter second-order polynomial fit to experimental data using Eq. 4 with the parameters in Table I. The root-mean-square deviation of the calculated coefficients of expansion, indicated with blue dashed lines, is $8.9 \times 10^{-6}/\text{K}$. The Pearson- r for this fit is 0.80.

this model drives the predicted CTE upward.

The CTE of KI is underestimated. While it has the rocksalt structure, with the corresponding $\sigma_c/\langle c \rangle = 0$, its mass ratio is 0.3 and volume ratio is 0.59, which cause the model to predict the lower value.

The essential dynamical contribution to thermal expansion cannot be fully captured by a static model, but we demonstrate that focusing on local properties that are linked to the dynamics, such as open space, bond coordinations, and atomic masses, provides a glimpse into these thermal motions for a range of different materials. The present model reveals trends in CTE values without specific descriptors to characterize the flexibility of A - B - A bond angles to bend nor the rigidity of polyhedral atom groups, which are frequently cited as important contributors to thermal expansion.

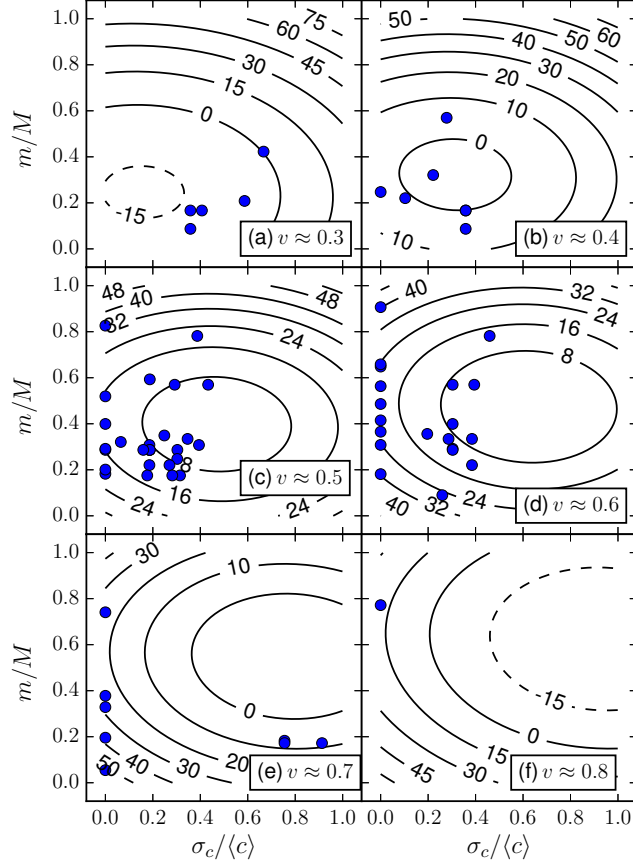


FIG. 4. (Color online) Contour plots showing the dependence of the calculated CTE_{calc} upon $\sigma_c/\langle c \rangle$ and m/M at fixed volume ratios v , as indicated. The circles plotted display the descriptor values for the materials used in the fit. The volume ratios for the data points displayed in each panel fall within ± 0.05 of the value of v indicated in each panel.

IV. CONCLUSION

The thermal expansion properties of solids emerge from the dynamics of ions and the bonds that join them. As a result, accurate theoretical prediction of thermal expansion is only possible with careful inclusion of the appropriate quantum mechanical considerations. These time-consuming calculations are a barrier to high-throughput searches of materials for candidates that possess particular thermal expansion characteristics. By encoding the relevant physics into simple descriptors, we have demonstrated that it is possible to ap-

proximate the thermal expansion coefficient of a variety of materials, including ionic binary compounds, perovskites, silicates, and other oxides by considering only the crystal structure of the material, the atomic masses, and the ionic radii of the atoms that compose it. These descriptors provide guidance for the search for new materials capable of mitigating thermal expansion in devices. Additional features that may prove important to this investigation include properties of the electronic structure of materials in, for example, magnetically driven NTE.

Appendix:

Table II lists the sources of structures and CTE used in this work.

TABLE II: All structural data used in this work are found in either the Crystal Online Database (COD) or in the Inorganic Crystal Structure Database (ICSD). Each material is listed with its database index. CTE values are listed with their data sources indicated. When a material is in a phase that is stable only above room temperature, this is indicated with the (high T) label. The volume ratio v is evaluated as described in the text.

Material	COD	ICSD	CTE ($10^{-6}/\text{K}$)	v
ScF ₃		261068	-14.00^{33}	0.335
Cr ₂ Mo ₃ O ₁₂ (high T)		418846	-9.30^{34}	0.351
CoZrF ₆ (high T)	1008795		-3.00^{35}	0.336
Al ₂ Mo ₃ O ₁₂ (high T)		80448	-2.83^{34}	0.364
Sc ₂ W ₃ O ₁₂		50941	-2.20^{36}	0.315
Sc ₂ Mo ₃ O ₁₂		391467	-2.10^{37}	0.318
β -quartz		89289	-1.33^{38}	0.526
LiAlSiO ₄	9011469		-0.40^{39}	0.443
Zn ₂ GeO ₄	9014631		0.00^{40}	0.367
Be ₃ Al ₂ Si ₆ O ₁₈	9014166		1.00^{41}	0.417

Continued on Next Page...

TABLE II – Continued

Material	COD	ICSD	CTE ($10^{-6}/\text{K}$)	ν
BN	9008834		1.15 ⁴²	0.821
Al ₂ W ₃ O ₁₂	1522201		2.20 ³⁶	0.360
AlN		54697	2.56 ⁴²	0.491
Cr ₂ FeO ₄	9007325		3.30 ³⁹	0.545
GaN	1010168		3.37 ⁴³	0.468
ZrSiO ₄	1011265		4.10 ³⁹	0.492
KNbO ₃	4119149		5.00 ⁴¹	0.736
FeAl ₂ O ₄	9006315		5.20 ³⁹	0.527
Fe ₃ Al ₂ Si ₃ O ₁₂	9006111		5.27 ³⁹	0.558
HfO ₂	1528988		5.27 ³⁹	0.550
MgCr ₂ O ₄	9007310		5.50 ³⁹	0.512
Be ₂ SiO ₄	9005857		5.60 ³⁹	0.510
Mn ₃ Al ₂ Si ₃ O ₁₂	9007701		5.73 ³⁹	0.555
Mg ₃ Al ₂ Si ₃ O ₁₂	9001685		6.63 ³⁹	0.565
NaCrSi ₂ O ₆	1531195		6.80 ³⁹	0.544
MgFe ₂ O ₄	9003592		6.83 ³⁹	0.483
Ca ₃ Fe ₂ Si ₃ O ₁₂	9010061		6.87 ³⁹	0.537
Fe ₃ O ₄	9009768		6.87 ³⁹	0.482
ZrO ₂	9007485		7.07 ³⁹	0.537
BeO	9015790		7.30 ⁴²	0.598
LiAlSi ₂ O ₆	9004744		7.40 ³⁹	0.510
MgGeO ₃	9000958		7.47 ³⁹	0.464
Al ₂ SiO ₅	9003990		7.60 ³⁹	0.466
TiO ₂	9015662		7.90 ⁴¹	0.543
BeAl ₂ O ₄	9005861		7.93 ³⁹	0.609
NaAlSi ₂ O ₆	9000344		8.23 ³⁹	0.553
Ca ₃ Al ₂ Si ₃ O ₁₂	9002686		8.30 ⁴⁴	0.563
SrZrO ₃	1528398		8.77 ⁴⁵	0.504
NaAlSi ₃ O ₈	9000526		8.93 ³⁹	0.400
ScAlO ₃	9008279		9.00 ³⁹	0.589
TiFeO ₃	1011033		9.30 ³⁹	0.539
SrTiO ₃	9006864		9.40 ⁴⁵	0.680
BPO ₄	1010299		9.40 ⁴⁶	0.480
Mo ₃ Fe ₂ O ₁₂	1524203		9.70 ³⁴	0.349
CaGeO ₃	9000904		10.37 ³⁹	0.618

Continued on Next Page...

TABLE II – Continued

Material	COD	ICSD	CTE ($10^{-6}/\text{K}$)	ν
Mg ₂ GeO ₄	9010486		10.70 ³⁹	0.541
MgAl ₂ O ₄	9007121		10.84 ⁴⁷	0.533
MgF ₂	9007534		11.00 ⁴¹	0.489
NaNbO ₃	1011064		11.00 ⁴¹	0.659
FeO	9009766		11.30 ³⁹	0.537
MnO	1514118		11.50 ³⁹	0.517
Bi ₂ Se ₃	1530736		13.67 ⁴⁸	0.750
SrO	7200689		13.72 ⁴⁹	0.524
CaO	9006717		13.80 ⁵⁰	0.509
MgO	9006758		15.70 ⁵¹	0.565
CaTiO ₃	9013383		25.00 ⁴¹	0.579
AgCl	9011666		32.90 ⁴⁹	0.668
LiF		181799	34.00 ⁴⁹	0.589
NaMgF ₃	9010943		34.00 ⁴¹	0.566
AgBr	9011682		34.10 ⁴⁹	0.712
NaF	9007457		36.00 ⁴⁹	0.547
RbCl	8103714		36.00 ⁴⁹	0.551
KF	9008652		36.70 ⁴⁹	0.570
KCl		165593	38.30 ⁴⁹	0.551
NaCl		165592	40.00 ⁴⁹	0.575
LiCl	9008665		44.00 ⁴⁹	0.669
KI	9009735		45.00 ⁴⁹	0.586
NaI	9008681		48.30 ⁴⁹	0.637
LiI	9008669		59.00 ⁴⁹	0.735

ACKNOWLEDGMENTS

This work has been supported by the Department of Energy Office of Basic Energy Sciences, under grant number DE-FG02-07ER46431. Computational support was provided

by the National Energy Research Scientific Computing Center (NERSC).

* joseph.schick@villanova.edu

- ¹ C. Lind, *Materials* **5**, 1125 (2012).
- ² J. Chen, L. Hu, J. Deng, and X. Xing, *Chem. Soc. Rev.* **44**, 3522 (2015).
- ³ T. A. Mary, J. S. O. Evans, T. Vogt, and A. W. Sleight, *Science* **272**, 90 (1996), <http://www.sciencemag.org/content/272/5258/90.full.pdf>.
- ⁴ A. K. A. Pryde, K. D. Hammonds, M. T. Dove, V. Heine, J. D. Gale, and M. C. Warren, *J. Phys.: Condens. Matter* **8**, 10973 (1996).
- ⁵ A. P. Ramirez and G. R. Kowach, *Phys. Rev. Lett.* **80**, 4903 (1998).
- ⁶ G. Ernst, C. Broholm, G. R. Kowach, and A. P. Ramirez, *Nature* **396**, 147 (1998).
- ⁷ R. Mittal and S. L. Chaplot, *Phys. Rev. B* **60**, 7234 (1999).
- ⁸ R. Mittal, S. L. Chaplot, H. Schober, and T. A. Mary, *Phys. Rev. Lett.* **86**, 4692 (2001).
- ⁹ D. Cao, F. Bridges, G. R. Kowach, and A. P. Ramirez, *Phys. Rev. Lett.* **89**, 215902 (2002).
- ¹⁰ D. Cao, F. Bridges, G. R. Kowach, and A. P. Ramirez, *Phys. Rev. B* **68**, 014303 (2003).
- ¹¹ J. N. Hancock, C. Turpen, Z. Schlesinger, G. R. Kowach, and A. P. Ramirez, *Phys. Rev. Lett.* **93**, 225501 (2004).
- ¹² M. G. Tucker, A. L. Goodwin, M. T. Dove, D. A. Keen, S. A. Wells, and J. S. O. Evans, *Phys. Rev. Lett.* **95**, 255501 (2005).
- ¹³ V. Gava, A. L. Martinotto, and C. A. Perottoni, *Phys. Rev. Lett.* **109**, 195503 (2012).
- ¹⁴ F. Bridges, T. Keiber, P. Juhas, S. J. L. Billinge, L. Sutton, J. Wilde, and G. R. Kowach, *Phys. Rev. Lett.* **112**, 045505 (2014).
- ¹⁵ A. Sanson, *Chemistry of Materials* **26**, 3716 (2014), <http://dx.doi.org/10.1021/cm501107w>.
- ¹⁶ M. K. Gupta, R. Mittal, S. L. Chaplot, and S. Rols, *Journal of Applied Physics* **115**, 093507 (2014).
- ¹⁷ E. S. Božin, T. Chatterji, and S. J. L. Billinge, *Phys. Rev. B* **86**, 094110 (2012).
- ¹⁸ T. Chatterji, T. C. Hansen, M. Brunelli, and P. F. Henry, *Appl. Phys. Lett.* **94**, 241902 (2009).
- ¹⁹ C. W. Li, X. Tang, J. A. Muñoz, J. B. Keith, S. J. Tracy, D. L. Abernathy, and B. Fultz, *Phys. Rev. Lett.* **107**, 195504 (2011).
- ²⁰ P. Lazar, T. c. v. Bučko, and J. Hafner, *Phys. Rev. B* **92**, 224302 (2015).

- ²¹ G. D. Barrera, J. A. O. Bruno, T. H. K. Barron, and N. L. Allan, *Journal of Physics: Condensed Matter* **17**, R217 (2005).
- ²² M. T. Dove and H. Fang, *Reports on Progress in Physics* **79**, 066503 (2016).
- ²³ J. T. Schick and A. M. Rappe, *Phys. Rev. B* **93**, 214304 (2016).
- ²⁴ G. Bergerhoff, *Crystallographic Databases*, edited by F. H. Allan, G. Bergerhoff, and R. Sievers (International Union of Crystallography, 1987).
- ²⁵ A. Belsky, M. Hellenbrandt, V. L. Karen, and P. Luksch, *Acta Crystallographica Section B* **58**, 364 (2002).
- ²⁶ A. Merkys, A. Vaitkus, J. Butkus, M. Okulič-Kazarinas, V. Kairys, and S. Gražulis, *Journal of Applied Crystallography* **49**, 292 (2016).
- ²⁷ S. Gražulis, A. Merkys, A. Vaitkus, and M. Okulič-Kazarinas, *Journal of Applied Crystallography* **48**, 85 (2015).
- ²⁸ S. Gražulis, A. Daškevič, A. Merkys, D. Chateigner, L. Lutterotti, M. Quiros, N. R. Serebryanaya, P. Moeck, R. T. Downs, and A. Le Bail, *Nucleic Acids Research* **40**, D420 (2012).
- ²⁹ S. Gražulis, D. Chateigner, R. T. Downs, A. F. T. Yokochi, M. Quirós, L. Lutterotti, E. Manakova, J. Butkus, P. Moeck, and A. Le Bail, *Journal of Applied Crystallography* **42**, 726 (2009).
- ³⁰ R. T. Downs and M. Hall-Wallace, *American Mineralogist* **88**, 247 (2003).
- ³¹ R. D. Shannon, *Acta Crystallographica Section A* **32**, 751 (1976).
- ³² P. W. Sparks and C. A. Swenson, *Phys. Rev.* **163**, 779 (1967).
- ³³ B. K. Greve, K. L. Martin, P. L. Lee, P. J. Chupas, K. W. Chapman, and A. P. Wilkinson, *Journal of the American Chemical Society* **132**, 15496 (2010).
- ³⁴ A. Tyagi, S. Achary, and M. Mathews, *Journal of Alloys and Compounds* **339**, 207 (2002).
- ³⁵ J. C. Hancock, K. W. Chapman, G. J. Halder, C. R. Morelock, B. S. Kaplan, L. C. Gallington, A. Bongiorno, C. Han, S. Zhou, and A. P. Wilkinson, *Chemistry of Materials* **27**, 3912 (2015), <http://dx.doi.org/10.1021/acs.chemmater.5b00662>.
- ³⁶ J. Evans, T. Mary, and A. Sleight, *Journal of Solid State Chemistry* **133**, 580 (1997).
- ³⁷ J. S. Evans and T. Mary, *International journal of inorganic materials* **2**, 143 (2000).
- ³⁸ P. R. L. Welche, V. Heine, and M. T. Dove, *Physics and Chemistry of Minerals* **26**, 63 (1998).
- ³⁹ Y. Fei, “Mineral physics & crystallography: A handbook of physical constants,” (American Geophysical Union, 1995) Chap. 2-4.

- ⁴⁰ R. Stevens, B. F. Woodfield, J. Boerio-Goates, and M. K. Crawford, The Journal of Chemical Thermodynamics **36**, 349 (2004).
- ⁴¹ H. D. Megaw, Materials Research Bulletin **6**, 1007 (1971).
- ⁴² G. A. Slack and S. F. Bartram, Journal of Applied Physics **46**, 89 (1975).
- ⁴³ H. Iwanaga, A. Kunishige, and S. Takeuchi, Journal of Materials Science **35**, 2451 (2000).
- ⁴⁴ D. G. Isaak, O. L. Anderson, and H. Oda, Physics and Chemistry of Minerals **19**, 106 (1992).
- ⁴⁵ D. de Ligny and P. Richet, Phys. Rev. B **53**, 3013 (1996).
- ⁴⁶ S. Achary and A. Tyagi, Journal of Solid State Chemistry **177**, 3918 (2004).
- ⁴⁷ P. Samui, N. K. Gupta, S. Dash, N. D. Dahale, and Y. Naik, Journal of Thermal Analysis and Calorimetry **115**, 1289 (2013).
- ⁴⁸ X. Chen, H. D. Zhou, A. Kiswandhi, I. Miotkowski, Y. P. Chen, P. A. Sharma, A. L. Lima Sharma, M. A. Hekmaty, D. Smirnov, and Z. Jiang, Applied Physics Letters **99**, 261912 (2011).
- ⁴⁹ S. Kumar, Proceedings of the National Institute of Sciences of India: Physical Sciences **25**, 364 (1959).
- ⁵⁰ Z.-H. Fang, Int J Thermophys **36**, 1577 (2015).
- ⁵¹ I. Suzuki, Journal of Physics of the Earth **23**, 145 (1975).